A Lagrangian Transport Model Applied to two Different Brackish Systems: the Baltic Sea and the Guadalquivir River

M. Toscano-Jiménez [1], J.M. Abril [2]

[1] E.T.S. de Ingeniería, University of Seville. 41092, Isla de la Cartuja, Seville, Spain. mtoscano@esi.us.es
[2] E.T.S.I. Agronómica, University of Seville. 41013, Crta. Utrera km.1, Seville, Spain. jmabril@us.es

ABSTRACT

This paper presents a numerical model for the transport of the nuclear contamination and other passive particles in the ocean. As a consequence of the Chernobyl accident (April, 26th, 1986), the radioactive plume drift over many countries in Europe, and after some days, the Baltic Sea became the most contaminated ecosystem beyond the Soviet Union. Our Dispersion Model has been validated in this system in order to be useful in other oceanic scenarios affected by radioactive fallout in the future. These investigations could be an interesting tool to predict and minimize the ecological and economical impacts of future accidents and can also be extended to non-nuclear contamination problems such as: oil accidents, chemical contamination, nutrients dynamics and other ecological problems.

A new application devoted to the Guadalquivir River has been implemented with the methods used and validated for the Baltic Sea. This transport model is a first step for future applications to passive particles problems such as nutrients, chemical contamination, metals, suspended sediments, etc., or other active parts like salt and fresh water. A deeper knowledge on the Guadalquivir river estuary is being demanding for many socioeconomic and ecological applications in the future.

I. INTRODUCTION

A previous Two-Scales Diffusion Model have been published elsewhere ([13], [14]), and being validated in the Baltic using data from the Chernobyl fallout. That model used an Eulerian scheme, and measured ^{137}Cs concentrations in seawater during October 1986 were stated as initial conditions for the numerical problem. The model solved the time evolution of concentrations for a 10 months period, and the predicted values were compared with the measured concentrations at such a date. The vertical gradients of radioactivity, five months after the fallout, were as low as the mean integrated advective velocity in the water column. These two points did not allow an important advection of the centroide of the two main radioactive spots in the Baltic, being their dynamics mainly governed by diffusive processes. The aim of this work is to present an Advection-Diffusion Model for the Baltic Sea, and to validate it under advective dynamics during the first months after the accident, when the wind-induced currents could drift some hundreds of km the centroide of the first radioactive spot detected in the Baltic Sea. Another goal of this work is to apply this methodology to simulate the dispersion of the salinity in the Guadalquivir Estuary.

II. METHODS

A. The Monte Carlo Method

In this work we used a Lagrangian numerical model for dispersion which evaluates the path of a discrete number of tracer particles. The main advantages are:

(a) It produces good results for problems involving high spatial gradients in tracer concentrations.
(b) It avoids the problem of numerical dispersion which affect the finite difference scheme working with the Eulerian method.

This approach allows to study the dispersion of conservative tracers ([6], [8]) following accidents or planned releases of different kinds of pollutants.

A basic outline of the movements of each particle is given by

$$\vec{r}(t+\Delta t) = \vec{r}(t) + \vec{v}(t)\Delta t \tag{1}$$

$$\vec{v} = \vec{v}^{\,m} + \vec{v}' \tag{2}$$

where $\vec{v}^{\,m}$ is the advective velocity and $\vec{v}'$ the diffusion velocity. The Cartesian components of $\vec{v}'$ will be calculated with a random distribution ([4]):

$$\left|v'_x\right|_{\max} = \left|v'_y\right|_{\max} = \sqrt{\frac{6K_h}{\Delta t_h}} \tag{3}$$

where K_h is the horizontal diffusion coefficient and Δt_h the time step. The calculations ([14]) have been done with a MATLAB random code:

$$v_x' = \sqrt{\frac{6K_h}{\Delta t_h}}\mathrm{RAN}_x \qquad v_y' = \sqrt{\frac{6K_h}{\Delta t_h}}\mathrm{RAN}_y \qquad (4)$$

where RAN_x and RAN_y are random numbers generated between -1 and +1. In an analogous way for the vertical diffusion velocity:

$$\left|v_z'\right|_{\max} = \sqrt{\frac{2K_v}{\Delta t_v}} \qquad v_z' = \sqrt{\frac{2K_v}{\Delta t_v}}\mathrm{RAN}_z \qquad (5)$$

B. Method validation: 1D Advection-Diffusion

The diffusion of an spot of initial density A_o , length h, in a one-dimensional fluid with a constant advection velocity, v, has been used as calibration function, since the known analytical solution can be compared against the numerical one:

$$\left\{\begin{array}{l} \text{1-D Calibration functions:} \\ A(x',t) = \dfrac{A_o}{2}\left[erf\left(\dfrac{x'+h/2}{\sqrt{2}\sigma_x(t)}\right) - erf\left(\dfrac{x'-h/2}{\sqrt{2}\sigma_x(t)}\right)\right]; \\ with: \quad x = x' + vt \quad ; \quad \sigma_x(t) = \sqrt{2K_x^{dif}t} \quad ; \\ erf(z) = \dfrac{2}{\sqrt{\pi}}\int_0^z e^{-x^2}dx \end{array}\right\} (6)$$

Figures 1 and 2 show the corresponding results using, respectively, N=10^4, and, $N = 36 \times 10^4$ (the number of Lagrangian tracer particles). In both cases, the initial density of the spot was A_o=N/h

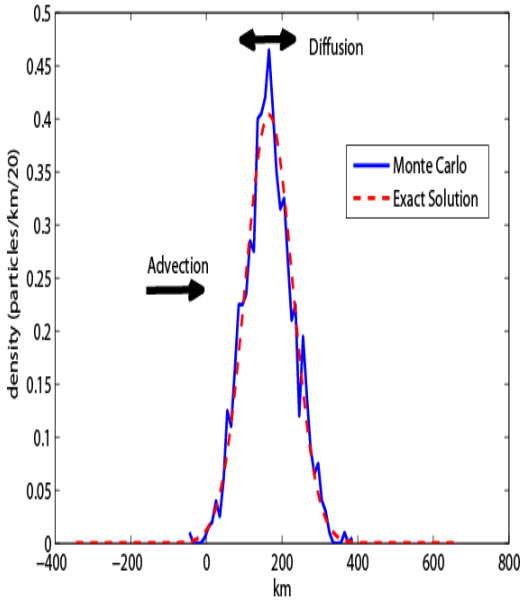

Figure 1. Simulation with N = 10000 particles, h = 20km, K_x = 250m^2 s^{-1}, v = 2cm/s , and 90 days of transport.

Deviations of the numerical fluctuations with respect to the exact solution are lower in the second case, and they satisfy the known statistical relationship

$$\left\{\begin{array}{l} \text{Lagrangian fluctuations: } \varepsilon_i \equiv \dfrac{\Delta N_i}{N_i} \\ \Delta N_i \propto \sqrt{N_i} \quad \Rightarrow \quad \varepsilon_i \propto 1/\sqrt{N_i} \end{array}\right\} \qquad (7)$$

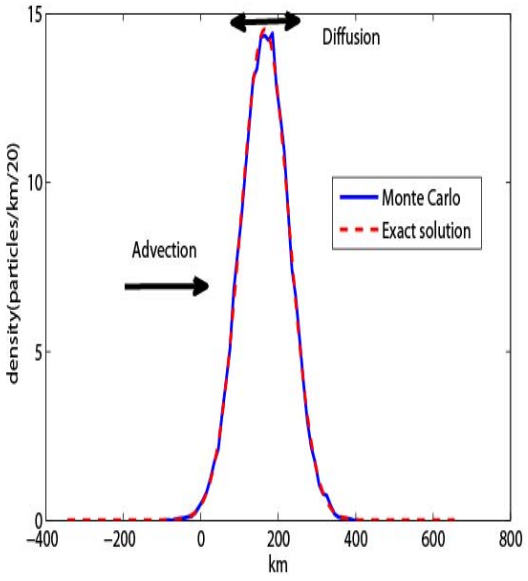

Figure 2. Simulation with N=36×10^4 particles, h=20km, K_x=250m^2 s^{-1}, v=2cm/s , and 90 days of transport.

The validation test has been extended to a two-dimensional problem for which analytical solutions can be stated, producing reasonable good results (not shown):

$$\left\{\begin{array}{l} \text{2-D Calibration functions:} \\ A(x,y,t) = \dfrac{A_o}{4}\left[erf\left(\dfrac{x+h/2}{\sqrt{2}\sigma_x(t)}\right) - erf\left(\dfrac{x-h/2}{\sqrt{2}\sigma_x(t)}\right)\right]\cdot \\ \left[erf\left(\dfrac{y+h/2}{\sqrt{2}\sigma_y(t)}\right) - erf\left(\dfrac{y-h/2}{\sqrt{2}\sigma_y(t)}\right)\right]; \\ with: \sigma_x(t) = \sqrt{2K_x^{dif}t} \quad ; \\ \sigma_y(t) = \sqrt{2K_y^{dif}t} \quad ; erf(z) = \dfrac{2}{\sqrt{\pi}}\int_0^z e^{-x^2}dx \end{array}\right\} (8)$$

III. APPLICATIONS

A. 3-D MODEL FOR THE BALTIC SEA. Wind blowing from the South.

A 3-dimensional numerical model has been adapted to the bathymetry of the Baltic Sea. The numerical models ([1] ,[3]) solved the hydrodynamic of the Baltic Sea under the forcing of winds. These results served us to implement a simplified 3D velocity field for the steady-state water circulation (Fig. 3).

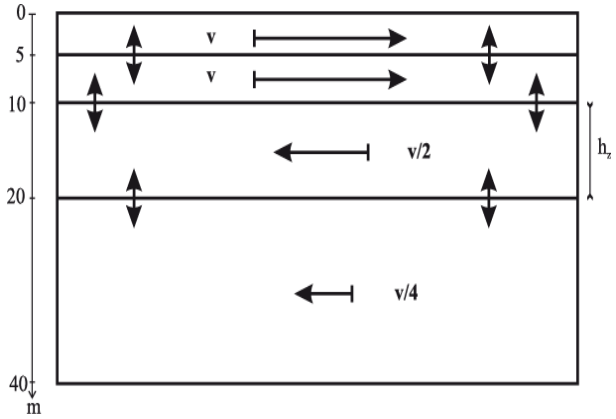

Figure 3. Vertical profile for the horizontal advective velocities in a four layers model. The mean advective velocity integrated in the four layers is null.

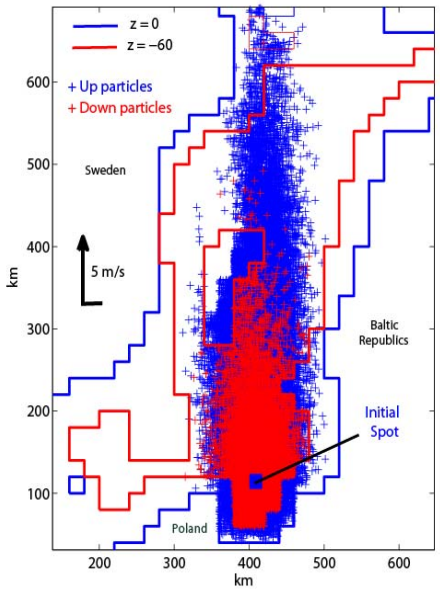

Figure 4. 3-D dispersion pattern of a hypothetical spot covering the surface layer of a grid-cell 20km×20 km after 90 days of transport forced by a wind of 5 m s^{-1} blowing from the South. $N = 25 \times 10^4$ particles, $K_v = 4 cm^2 s^{-1}$, $K_h = 40 m^2 s^{-1}$. The figure shows distributions up and down the picnocline.

The magnitude of the water current at the surface layer of the Ocean was fixed as being a 2% of the wind speed measure 10 m above MSL ([9]). In the first modeling exercise we used a wind speed of 5 m s^{-1} blowing from the South. Figure 4 shows the 3D dispersion pattern of a hypothetical spot under these forcing conditions.

The resulting flux through the pycnocline was consistent with the required to maintain the existing levels of salinity on each side of the pycnocline ([12]). According to this study 2.5% of the upper fluid crosses the pycnocline each year, while our calculations show amounts ranging from 2% up to 3.5 %. The required CPU time to run the model was 7 minutes in a standard personal computer.

In a second modeling exercise, we keep the previous settings from Fig. 4 and varied the K_v value to simulated different diffusion scenarios.

Results are shown in Fig. 5 for three values of K_v and after 90 days of transport. En each case we plot the density of particles in the upper (0-5 m) and lower (below 60 m) water layers. The position of the peak is drifted by winds, and the Gotland Island (covering the coordinates interval 300< y <400 km) partially retains the pollution upwind. A similar effect is produced by the strait of the Aland Islands (500< y <700 km), close to the Gulf of Bothnia.

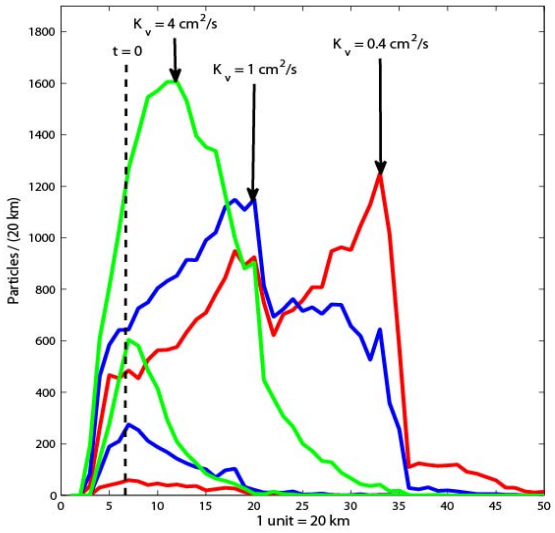

Figure 5. Horizontal profiles for the spot for different values of *Kv* after 90 days of transport, under the physical settings used in Fig. 4. Particle concentrations refers to the upper (0-5 m) and lower (below 60 m) ocean layers.

From Fig. 5 it is possible to estimate the contribution of the Shear effect to the global diffusion:

$$\left\{ \begin{array}{l} \text{Shear Effect:} \qquad K_{sh} \equiv v_{sh}^2 T_{sh} \\ v_G \equiv \dfrac{mv + mv + 2m(-v/2)}{4m} = \dfrac{v}{4} \\ v_{sh} \equiv v' = v - v_G = \dfrac{3v}{4} \end{array} \right\} \qquad (9)$$

where v_{sh} are the associated fluctuating velocities, and T_{sh} is the associated time-scale.

Taking this last as the time required by a fluid volume to be advected in the vertical direction through two adjacent ocean layers of h_z =10 m thickness ($l_z = h_z$), then

$$\left\{ \begin{array}{l} K_z \equiv \dfrac{l_z^2}{T_z} \quad , \; T_z = T_{sh} \; , \; l_z = h_z \\ (9) \;\Rightarrow\; K_{sh} \equiv v_{sh}^2 T_{sh} = \dfrac{9}{16} \dfrac{v^2 h_z^2}{K_z} \\ K_{sh} \quad \propto \quad \dfrac{1}{K_z} \end{array} \right\} \qquad (10)$$

The diffusion coefficient due to the Shear effect is inversely proportional to the vertical diffusion coefficient, as it can be seen in Figure 5.

In other modeling exercise we kept the same physical settings from Fig. 4, with a fixed value K_v= 4cm^2 s^{-1}, and we varied the time of simulation from 10 up to 120 days.

Results are shown in Figs. 6 and 7. We note as after 50 days, the advective drift of the plume stops after what pure diffusion dominates.

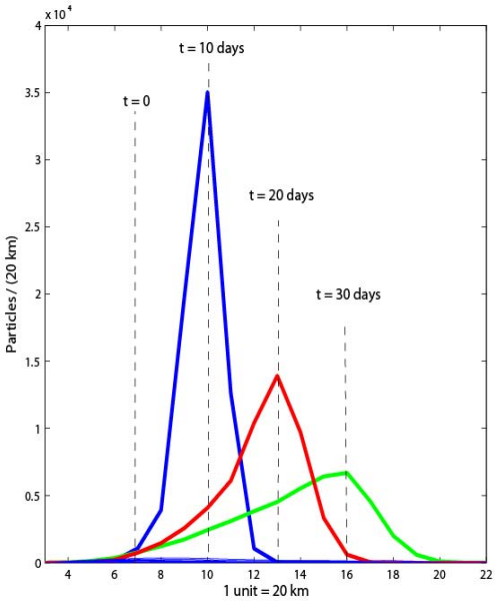

Figure 6. Dispersion of the spot for K_v=4cm^2 s^{-1} after 10, 20 and 30 days of transport. The density of particles in the surface layer is being represented in the axis Y.

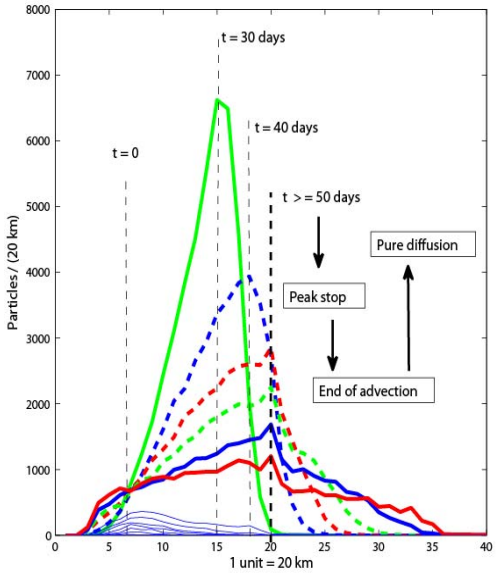

Figure 7. Dispersion and peak stop for K_v=4cm^2 s^{-1}. The density of particles in the surface layer is being represented in the axis Y.

This fact can be explained by the 3-D structure of the water currents induced by winds blowing from the South in this region of the Baltic Sea. They produce surface water currents (0-10 m) northwards directed, with reverse water circulation in deeper layers (10-40 m). Initially the spot is assumed to be located in the upper water layer, and then, its centroide moves with surface currents. As result of the vertical diffusion, the multilayer structure with reverse advection produces a null averaged value for the velocity of the centroide.

The time required to reach this null advective velocity can be related with the time involved in the effective mixing of the 0-40 m ocean layer, which can be evaluated from Eq. 10:

$$\left\{ \begin{array}{l} K_z \equiv \dfrac{l_z^2}{T_z} \quad ; \quad l_z = 20m \quad , \quad K_z = 1cm^2/s \\ \\ T_z \approx 46 \text{ days} \end{array} \right\} \qquad (11)$$

This is in good agreement with our model results.

B. MODELLING THE FATE OF A RADIOACTIVE SPOT IN THE GULF OF FINLAND.

Few days after the Chernobyl accident (April 26th, 1986), high ^{137}Cs concentrations were measured in the Gulf of Finland ([2]). In June 1986, the centroide of the radioactive spot was located North of the central part of this region of the Baltic Sea (Fig. 8). New measurements carried out in August 1986 revealed that the maximum activity concentration had displaced about 100 km to the South-West ([7]).

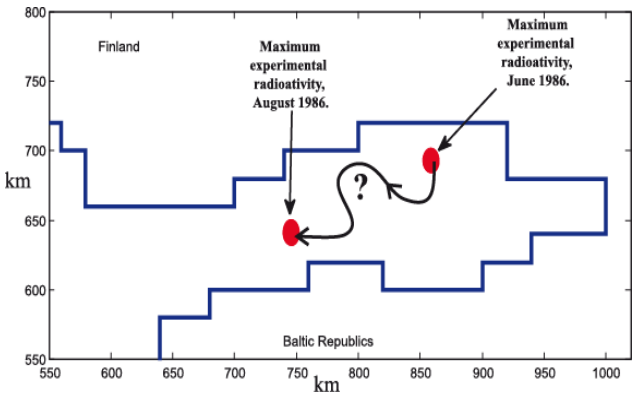

Figure 8. Scheme of the advection of the radioactive spot, summer 1986.

This advective displacement is compatible with the water circulation forced by the prevailing winds. Monthly values of NAO (North Atlantic Oscillation), revealed extreme values of -4 in summer 1986 ([5]), which resulted in dominant winds blowing from North and East in Northern Europe (Radziejewska T. et al., 2004).

In our modeling exercise the initial time was fixed at June the 15th, and the time of simulation ended in August the 15th. The water circulation was implemented from the mean summer currents produced with the hydrodynamic model of SMHI ([1]). A realistic constant value of K_h =100 m^2s^{-1} was adopted for the horizontal diffusion coefficient. Taking into account the relative vertical stability of the Baltic Sea in summertime, the vertical diffusion coefficient was varied within the following interval

$$K_v \in [0.2, 20]\,\mathrm{cm}^2\mathrm{s}^{-1} \qquad (12)$$

Its final value will be selected attending to the best description of the observed fate of the radioactive spot.

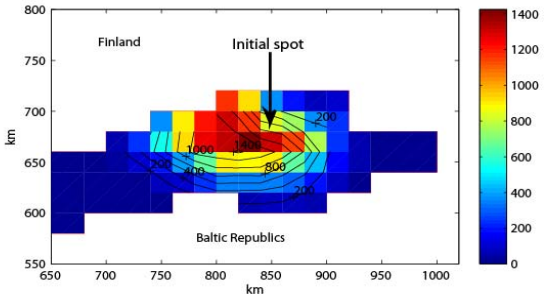

Figure 9. Model results for K_v = 20 cm^2s^{-1}. See text for physical settings and model parameters.

As initial conditions, the spot was located in the surface layer of the grid cell located at model coordinates [840,680] km , and it was assumed to be uniformly distributed within the grid-cell area (20km×20km). The Monte Carlo method was then applied with $N = 25\times10^4$.

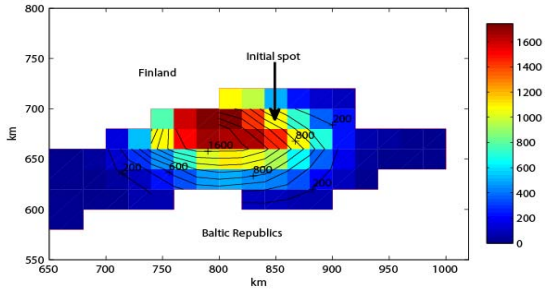

Figure 10. As Fig. 9, with K_v = 6 cm^2s^{-1}

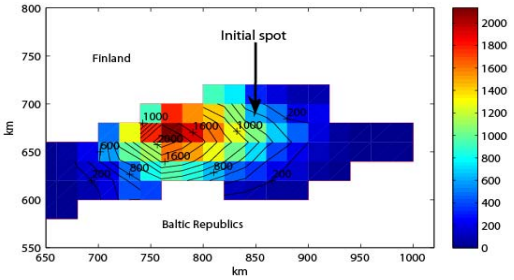

Figure 11. As Fig. 9, with K_v = 2 cm^2s^{-1}

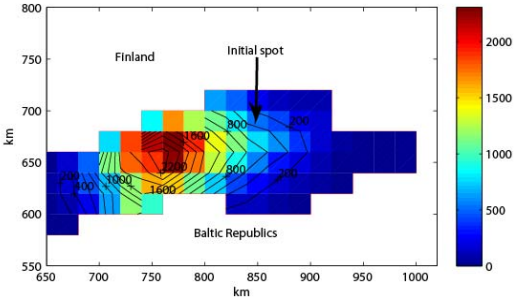

Figure 12. As Fig. 9, with K_v = 1 cm^2s^{-1}

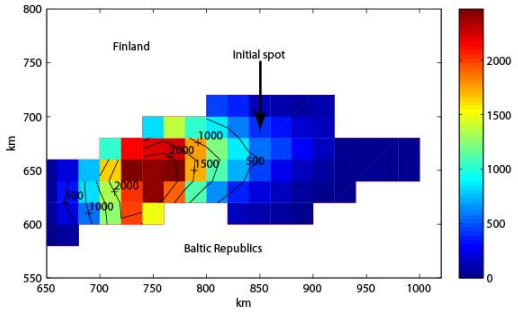

Figure 13.As Fig. 9, with K_v = 0.5 cm^2s^{-1}

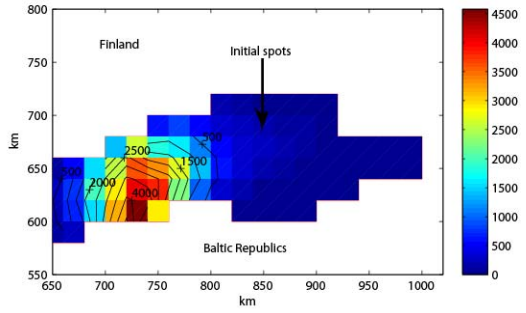

Figure 14. As Fig. 9, with $K_v = 0.2$ cm^{2}s^{-1}

Although K_v =0.2 cm^{2}s^{-1} produces results being apparently compatible with observations in August 1986, the ulterior fate of the plume does not correspond with the observational data. Thus, the model predictions is a further advective transport, as shown in Fig. 15, while measurements ([7]) revealed a virtual detention of the spot at its location in August 1986. From our model results, both K_v = 2 cm^{2}s^{-1} and K_v = 1 cm^{2}s^{-1} are producing a reasonable description of the fate of the radioactive spot, compatible with observations ([2],[7]).

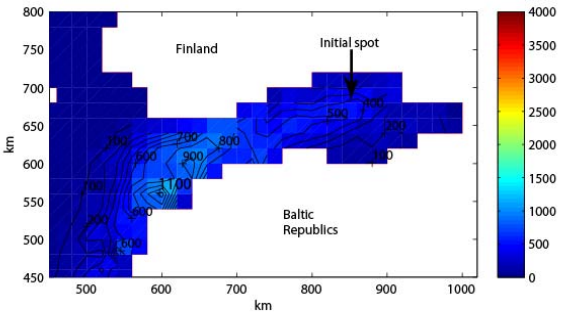

Figure 15. As in Fig. 9, with $K_v = 0.2$ cm^{2}s^{-1} and a simulation time of 150 days. The spot continues its advective drift, in contradiction with observations.

C. MODELING HORIZONTAL GRADIENTS OF SALINITY IN THE GUADALQUIVIR RIVER.

The Guadalquivir is the second longest river in Spain (after the Tagus), and the longest in Andalusia. It is 657 kilometers long and drains an area of about 58,000 square kilometers (2/3 of the andalusian total area), flowing into the Gulf of Cádiz, in the Atlantic Ocean. The marshy lowlands at the river's end are known as "Las Marismas". It borders Doñana National Park reserve.

The Guadalquivir River is the only great navigable river in Spain (currently it is navigable to Seville). The estuary is 110 km long, and the tidal influence ends at the dam in Alcalá del Río. Salinity along the Guadalquivir estuary is governed by the tidal intrusion of marine water and the main freshwater inputs.

Figure 16. Satellite image (NOAA): the blue line represents the stretch of the Guadalquivir estuary from the Atlantic Ocean to Seville (kilometer 90).

The typical tidal range at its mouth is about 2 meters in spring tides, and about its half for neap tides. Water currents are relatively high, of the order of 1 ms^{-1} during spring tides. Fresh water inputs through the dam in Alcalá del Río is variable along the year, with an annual average value of 50 m^{3}s^{-1}, and typical values of 20-30 m^{3}s^{-1} in summer time. These last values guaranties acceptable salinity levels in the central area of the Guadalquivir estuary, devoted to intensive agriculture productions. In rainy periods, the freshwater inflow ranges between 50 and 100 m^{3}s^{-1}.

Concerning the tidal regimen, the estuary, three different regions can be distinguished [11]:

(a) Region hyper-synchronous (0-15km): friction dominates and the range of tide falls within this range.
(b) Region synchronous (15-45km): The friction compensates the convergence and the tidal amplitude remains almost constant.
(c) Region hypo-synchronous (45-110km): amplitude grows by convergence and reflection at the dam.

The cross-sectional area, *a(x)*, the top wide, *b(x)* and the mean depth *h(x)* can be parameterized as a function of the distance *x* (in km) to the river mouth, as follows [11]:

$$\left\{\begin{array}{l} a(x) = a_0 \exp(-x/\lambda) \;,\; a_0 = 5840 m^2 \;,\; \lambda = 60 km \\ b(x) = b_0 \exp(-x/\mu) \;,\; b_0 = 795 m \;,\; \mu = 66 km \\ h(x) = h_0 \;,\; h_0 = 7.1 m \end{array}\right\} \quad (13)$$

A 1-D Lagrangian numerical model has been implemented for the Guadalquivir estuary to study horizontal gradients of salinity (averaged values over semidiurnal and spring-neap tidal cycles).

A detailed description of the hydrodynamics of the Guadalquivir estuary can be found elsewhere [11]. Particularly, the effective horizontal diffusion coefficient K_x has been studied as a function of the tidal currents, the friction coefficient, and the freshwater inputs. As a conclusion, the following range of variability has been established [11]:

$$150\ \mathrm{m^2 s^{-1}} \le K_x \le\ 1000\ \mathrm{m^2 s^{-1}} \qquad (14)$$

The 1D-Lagrangian model uses a number of tracer particles proportional to the salinity, given this last in PSU units. The 1-D approach seems to be reasonable for this particular scenario because of the dredging of the river, the drainage of marshlands, and other human interventions in the past half century.

The spatial discretization of the model uses Δx= 1 km, with Δt = 1 hour. As a first approach, the residual circulation was estimated assuming a mean flow at each section equal to the freshwater input at the upstream boundary.

As initial conditions, a number of particles $N(x)=100\ S\ \Delta x$, was ascribed as each sector, being S the salinity. As boundary condition and the estuary mouth, a compartment has been including, reproducing the open sea by means of a fast and homogenous mixing condition. By imposing the above forcing conditions, and after a transitory regimen lasting few days, a steady state situation is reached. A reasonable agreement with observational data has been achieved with the following parameterization of the effective diffusion coefficient:

$$K_x(x) = K_0\left(1-\gamma\frac{x}{l_E}\right)^2 \qquad (15)$$

where K_0 is the corresponding value for x = 0, γ is a free parameter to be fitted, and l_E is the length of the estuary.

Figure 17 shows the model results for the steady state distribution of salinity (in SPU units) obtained for a freshwater input Q = 25m^3/s, and they are compared against measured values [11].

Similarly, Fig. 18 shows the corresponding results for a freshwater input Q = 60 m^3/s

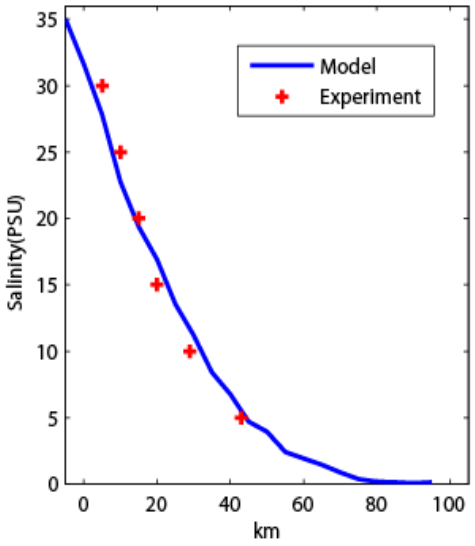

Fig. 17. Comparison against measured (averaged valyues over a semidiurnal and spring-neap tidal cycle) and computed steady-sate salinity values as a function of the distance to the estuary mouth. The freshwater input was Q = 25m^3/s (typical during dry periods), K_0 = 300m^2/s, γ = 3/4, and l_E = 110km.

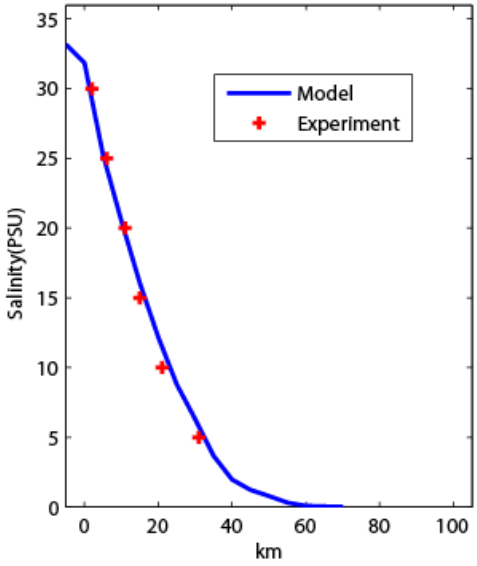

Figure 18. As Fig. 16, for a freshwater input Q = 60m^3/s (typical during rainy periods), K_0 = 600m^2/s, γ = 1/2, and l_E = 110km.

The reasonable agreement between model predictions and measured values provides the required support for this preliminary version of our 1-D Lagrangian dispersion model for the Guadalquivir estuary. Further improvements will include tidal oscillations, time-dependent diffusion coefficients, and a more detailed description of the estuarine hydrodynamics.

IV. CONCLUSIONS

This lagrangian transport model has been applied and validated to two different brackish systems: the Baltic Sea and the Guadalquivir River. Some advantages of these methods are the good results for problems involving high spatial gradients in tracer concentrations because they avoid the problems of the numerical dispersion which affect the Eulerian methods like Finite Difference and Finite Elements numerical techniques.

These investigations could be an interesting tool to predict and minimize the ecological and economical impacts of future accidents and can also be extended to non-nuclear contamination problems such as: oil accidents, chemical contamination, nutrients dynamics and other ecological problems.

REFERENCES

[1] L. Funkquist and L. Gidhagen. "A model for pollution studies in the Baltic Sea". *SMHI-Report RHO-39*, 1984

[2] Gritchenko, Z.G., Ivanova, L.M., Orlova, T.E., Tishkova, N.A., Toporkov, V.P., Tochilov I., 1989. Radiation situation in the Baltic Sea in 1986 in sea water and sediments. In: Three years observations of the levels of some radionuclides in the Baltic Sea after the Chernobyl accident. *Baltic Sea environment proceedings*, vol. 31, Helsinki, Finland, pp. 10-30.

[3] Jankowski A., 1983a. "An model H-N for the calculation of wind- and density- driven circulation in the Baltic Sea". Part I. Theoretical basis. Wind - driven circulation in the homogeneous Baltic Sea". *Oceanologia*, 1983, No. 14, 23-75.

[4] Jaun A., 2005. Numerical Methods for Partial Differential Equations. *Royal Institute of Technology*, Stockholm.

[5] Lehmann, A., Krauss,W., Hinrichsen, H.-H., 2002. "Effects of remote and local atmospheric forcing on circulation and upwelling in the Baltic Sea". *Tellus A*, 54, 299-316.

[6] Nakano M., Povinec P.P., 2003. **"**Oceanic general circulation model for the assessment of the distribution of 137Cs in the world ocean". *Deep Sea Research*, Part II, 50, pp. 2803-2816.

[7] Nies, H., 1989. The distribution of Chernobyl fallout over the Baltic Sea and its change during 1987 and 1988. In: Three years observations of the levels of some radionuclides in the Baltic Sea after the Chernobyl accident. *Baltic Sea environment proceedings*, vol. 31, Helsinki, Finland, pp. 31-51.

[8] Periañez, R. and Elliott, A.J., 2002. "A particle tracking method for simulating the dispersion of non-conservative radionuclides in coastal waters". *Journal of Environmental Radioactivity* 58, 13-33.

[9] Periañez R., 2005. *Modelling the Dispersion of Radionuclides in the Marine Environment*. An Introduction. Springer-Verlag Berlin Heidelberg, 2005.

[10] Radziejewska T., Chabior M., 2004. "Climatic and hydrological controls over the zoobenthos in a southern Baltic coastal lagoon". *Hydrobiologia*, 514, pp.171-181, 2004.

[11] J. Ruiz-Segura, M.A. Losada-Rodríguez, M.J. Polo-Gómez, S. Bramato, M. Díez-Minguito, 2010. *Propuesta metodológica para diagnosticar y pronosticar las consecuencias de las actuaciones humanas en el Estuario del Guadalquiv*ir. 2010.

[12] Svansson, A., 1980. "Exchange of water and salt in the Baltic and adjacent seas". *Oceanologica Acta* 3, 431-440.

[13] M. Toscano-Jimenez and R. García-Tenorio, "Modelling The Dispersion Of 137Cs In Marine Ecosystems With Monte Carlo Methods", *Nuclear Instruments And Methods B*, vol.213, pp.789-793, 2003.

[14] M. Toscano-Jimenez and R. García-Tenorio, "A Three-Dimensional Model For The Dispersion Of Radioactive Substances In Marine Ecosystems. Application To The Baltic Sea After The Chernobyl Disaster", *Ocean Engineering*, vol.31, pp.999-1018, 2004.